Nonlinear Science 4 (2025) 100031

Contents lists available at ScienceDirect

Nonlinear Science

journal homepage: www.elsevier.com/locate/nls

Research paper

Modeling the implications of seasonality and heterogeneous mean worm burden in Guinea-worm disease dynamics in dog population

Eva Lusekelo [a], Salamida Daudi [b], Mlyashimbi Helikumi [c], Steady Mushayabasa [d,e,*]

[a] University of Dodoma, College of Natural and Mathematical Sciences, Department of Mathematics & Statistics, P.O. Box 338, Dodoma, Tanzania
[b] National Institute of Transport, Faculty of Informatics and Technical Education, Department of Education and Mathematics, P.O. Box 705, Dar-es-Salaam, Tanzania
[c] Mbeya University of Science and Technology, Department of Mathematics and Statistics, College of Science and Technical Education, P.O. Box 131, Mbeya, Tanzania
[d] Harare Institute of Technology, P.O. Box BE 277, Belvedere, Harare, Zimbabwe
[e] University of Zimbabwe, Department of Mathematics & Computational Sciences, P.O. Box MP 167 Mount Pleasant, Harare, Zimbabwe

ARTICLE INFO

Keywords:
Guinea-worm disease
Dog population
Seasonality
Mean worm burden
Control strategies

ABSTRACT

Prior to 2012, it was believed that only humans could host Guinea-worm disease. Recent findings show that dogs also act as hosts. With the 2030 goal for eradicating Guinea-worm approaching, understanding dogs' roles is crucial. We develop a mathematical model to study seasonal Guinea-worm disease, focusing on dogs as primary hosts, given the low human cases. Our model includes seasonal variations, as previous studies indicate that disease prevalence is linked to seasonal fisheries. We also categorize infectious dogs based on their average worm burden. Our analysis examines how dog screening and tethering influence disease dynamics. Results indicate that both strategies can lower disease transmission. However, they may not be enough for total eradication on their own. Therefore, we suggest combining these methods with additional actions, like dog culling, to improve disease control.

1. Introduction

Neglected tropical diseases (NTDs) remain a major challenge in developing countries. According to estimates, there are approximately 1.7 billion individuals worldwide who are affected by NTDs [1]. Controlling and eliminating NTDs is closely linked to the Sustainable Development Goals [2]. In particular, Guinea-worm disease (GWD), which is caused by the nematode *Dracunculus medinensis*, is among the NTDs that are being targeted for elimination by 2030 [1]. As of today, the Carter Center's concerted efforts, which began in 1986, have shown exceptional success [1]. Reports show a reduction of over 99·9% from the 3.5 million human cases across 21 countries in Africa and Asia in 1986 to only 13 human cases in 2023 (9 in Chad, 2 in South Sudan, 1 in Cameroon, Mali and Central African Republic) [3].

However, as the transmission of GWD to humans has largely been interrupted, a new challenge has emerged. Historically, it was believed that humans were the primary and most common terminal host of GWD. However, the discovery in 2012 of a genetically identical worm in domesticated dogs (*Canis familiaris*) in Chad confirmed earlier accounts that animals can also serve as terminal hosts for GWD [4,5]. Recent reports indicate that animal infections have increased modestly, from 685 in 2022 to 713 in 2023 [3].

* Corresponding author at: University of Zimbabwe, Department of Mathematics & Computational Sciences, P.O. Box MP 167 Mount Pleasant, Harare, Zimbabwe.

E-mail addresses: lusekeloe@nm-aist.ac.tz (E. Lusekelo), daudisalamida81@gmail.com (S. Daudi), mhelikumi@yahoo.co.uk (M. Helikumi), steadymushaya@gmail.com (S. Mushayabasa).

https://doi.org/10.1016/j.nls.2025.100031
Received 6 December 2024; Received in revised form 8 May 2025; Accepted 9 May 2025
Available online 26 May 2025

Moreover, field reports indicate that dogs may experience varying levels of infection risk [6,7]. For instance, studies conducted between 2015 and 2018 revealed that a single dog can carry up to 79 worms [6]. Additionally, prior research suggests that the prevalence of GWD in dog populations is significantly influenced by seasonal variability in fishing activities [8]. As the target timelines approach, understanding the impact of seasonality and the heterogeneous mean worm burden within dog populations becomes increasingly important from both practical and theoretical perspectives. To that end, we present a mathematical model for GWD transmission that incorporate dogs as the only terminal host. The model also include the copepods and fish as intermediate hosts. The effects of seasonality are included in the model through assumptions regarding the time-dependence of some of the model parameters. In particular, we assume that larvae decay, disease transmission rates as well as the birth and mortality rates of intermediate hosts (copepods and fish) are periodic through the year.

Mathematical models are tools that can provide insight into the mechanisms that underlie the processes of disease spread and guide mitigation efforts [9]. Mathematical models proffer a low-cost mechanism for investigating biological processes and interventions for which experimental data may be scarce. A number of researchers have recently utilized mechanistic models to comprehend the transmission dynamics and control efforts for GWD (see, for example, [10–19]. Link and Donnay [10] as well as Adewole and Onifade [11] developed a GWD model that incorporate human and copepod population. Smith? et al. [12] utilized impulsive differential equations to investigate the effectiveness of chlorination on mitigating the spread of GWD in humans [12]. Netshikweta and Garira [13] developed a multiscale model for GWD using nonlinear ordinary differential equations (NODEs) to study the effect of intervention strategies on mitigating disease prevalence in humans. Their study suggested that treating water sources is the most effective strategy to control GWD. In the framework of Netshikweta and Garira, the dog population was not taken into account. To fill this gap in the work of Netshikweta and Garira, Engelhard et al. [18] developed a compartmental model that includes both humans and dogs. Both human and dog-focused interventions were included, such as burying fish entrails. Since more than 70% of the global dog population is free-ranging [20], it is essential to distinguish between free-ranging and non-free-ranging dogs in mathematical studies of GWD. Helikumi and Mushayabasa [19] developed a compartmental model for GWD transmission that incorporates both free-ranging and non-free-ranging dogs. Their study suggests that the elimination of GWD can be achieved if interventions target both FRDs and non-FRDs. Despite these efforts, the quantitative impact of seasonality and variability in the mean worm burden of the dog population on GWD transmission dynamics remains poorly understood.

The proposed mathematical framework summarizes the GWD cycle which begins when a adult female worm releases Stage 1 larvae into water. These larvae are consumed by copepods, and they undergo two molts and become Stage 3 larvae. The susceptible fish become infected when they consume infectious copepods. The terminal host (dogs) acquire infection by consuming infected fish. Once in the terminal host, the larvae are liberated, mating occurs, and the male worm dies. The pregnant female migrates towards the surface of the skin in the lower extremities where a painful blister is formed. In order to relieve the pain, the infected dog immerses the blister in water and the worm releases new larvae [21].

The study is organized as follows: In the next section, we introduce the mathematical model that describes the dynamics of GWD. We present the threshold dynamics, specifically computing the reproduction number, examining the global stability of the disease-free equilibrium, and investigating the existence of periodic solutions. In Section 3, we conduct numerical simulations to support our theoretical findings and assess the effectiveness of various control measures. Finally, we provide concluding remarks in Section 4.

2. Methods

2.1. Model derivation

In order to formulate the model, let $L(t)$ be the density of the larvae in the environment. We subdivide the dog population into four compartments: susceptible, exposed, lightly infected and heavily infected, the numbers of which at time t are denoted by $S_D(t)$, $E_D(t)$ and $I_{LD}(t)$ and $I_{HD}(t)$, respectively. Thus, the total dog population at any time t is denoted by

$$N_D(t) = S_D(t) + E_D(t) + I_{LD}(t) + I_{HD}(t). \tag{2.1}$$

Let $S_C(t)$, $E_C(t)$ and $I_C(t)$ be the number of susceptible, exposed and infectious copepods at time t, respectively. Thus, the total population of copepods at any time t is denoted by

$$N_C(t) = S_C(t) + E_C(t) + I_C(t). \tag{2.2}$$

Let $S_F(t)$ and $I_F(t)$ be the number of susceptible and infectious fish at time t, respectively. Thus, the total population of fish at any time t is given by $N_F(t) = S_F(t) + I_F(t)$. With these considerations, we shall explore the following system

$$\begin{aligned}
L'(t) &= \theta_D(t)(1-\phi_D)I_{LD}(t) + \theta_D(t)I_{HD}(t) - \mu_L(t)L(t),\\
S_C'(t) &= \mu_C(t)N_C(t) - \beta_{LC}(t)L(t)S_C(t) - \mu_C(t)S_C(t),\\
E_C'(t) &= \beta_{LC}(t)L(t)S_C(t) - (\mu_C(t)+\gamma_C)E_C(t),\\
I_C'(t) &= \gamma_C E_C(t) - \mu_C(t)I_C(t),
\end{aligned}$$

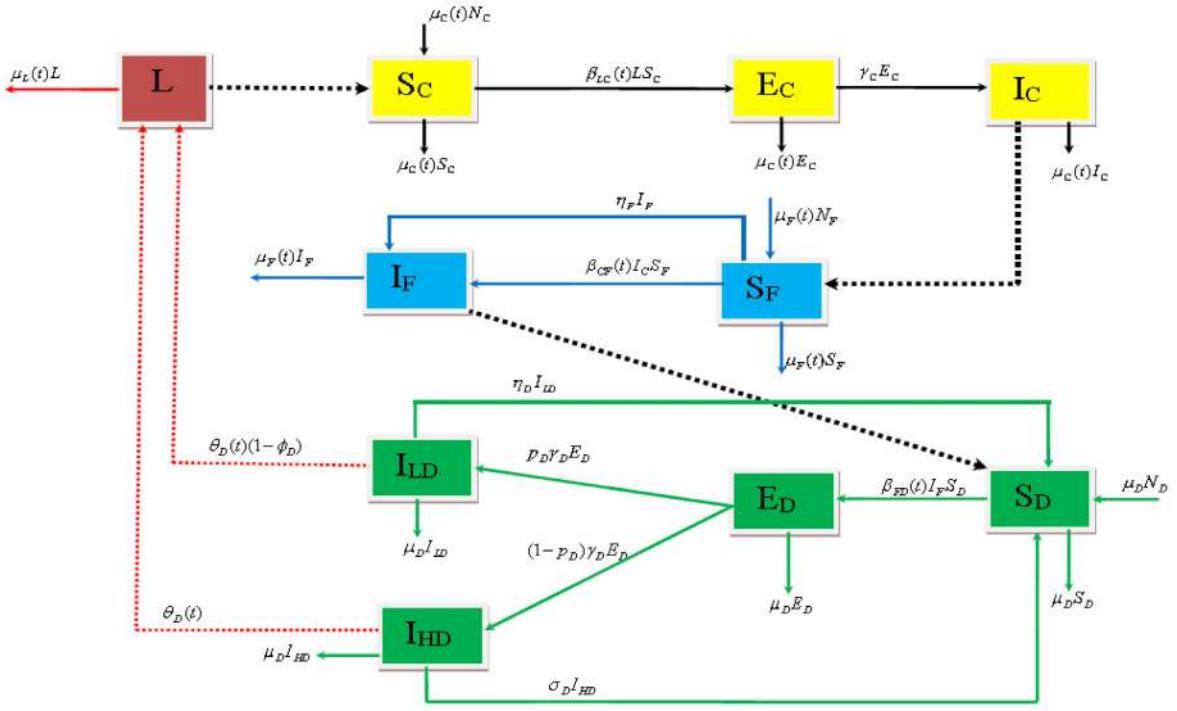

Fig. 1. A schematic diagram of GWD transmission for model (2.3).

$$
\begin{aligned}
S'_F(t) &= \mu_F(t)N_F(t) - \beta_{CF}(t)I_C(t)S_F(t) - \mu_F(t)S_F(t) + \eta_F I_F(t),\\
I'_F(t) &= \beta_{CF}(t)I_C S_F - (\mu_F(t)+\eta_F)I_F,\\
S'_D(t) &= \mu_D N_D(t) - \beta_{FD}(t)I_F(t)S_D(t) - \mu_D S_D(t) + \eta_D I_{LD}(t) + \sigma_D I_{HD}(t),\\
E'_D(t) &= \beta_{FD}(t)I_F(t)S_D(t) - (\mu_D+\gamma_D)E_D(t),\\
I'_{LD}(t) &= p_D\gamma_D E_D(t) - (\mu_D+\eta_D)I_D(t),\\
I'_{HD}(t) &= (1-p_D)\gamma_D E_D(t) - (\mu_D+\sigma_D)I_{HD}(t).
\end{aligned}
\tag{2.3}
$$

Here, time-dependent model parameters account for seasonal variability in GWD transmission. Parameter $\theta_D(t)$ denotes the shedding rate of larvae by infectious dogs; ϕ_D $(0 < \phi_D < 1)$ represents the reduction in the shedding rate of lightly infected dogs compared to heavily infected ones. $\mu_L(t)$ represents the mortality rate of larvae; $\mu_C(t)$ represents the birth and natural death rate of copepods; $\beta_{LC}(t)$ is the infection rate of copepods; $1/\gamma_C$ is the average molting time for the larvae. $\mu_F(t)$ denotes the birth and mortality rate of fish populations; $\beta_{CF}(t)$ and η_F are the infection and recovery rates of fish populations, respectively. μ_D is the birth and death rate of dogs; $\beta_{FD}(t)$ and γ_D represent the infection and incubation rates in dogs. Let p denote the proportion of exposed dogs that progress to the lightly infected group, with the remainder $(1-p)$ becoming heavily infected. Infectious lightly infected and heavily infected dogs recover at rates η_D and σ_D, respectively.

In order to mimic seasonal variations in GWD dynamics, we propose the following periodic functions:

$$
\begin{aligned}
\mu_C(t) &= \bar{\mu}_C(1+a\sin(\varphi t+\phi)), & \mu_L(t) &= \bar{\mu}_L(1+a\sin(\varphi t+\phi)),\\
\mu_F(t) &= \bar{\mu}_F(1+a\sin(\varphi t+\phi)), & \theta_D(t) &= \bar{\theta}_D(1+a\sin(\varphi t+\phi)),\\
\beta_{LC}(t) &= \bar{\beta}_{LC}(1+a\sin(\varphi t+\phi)), & \beta_{CF}(t) &= \bar{\beta}_{CF}(1+a\sin(\varphi t+\phi)),\\
\beta_{FD}(t) &= \bar{\beta}_{FD}(1+a\sin(\varphi t+\phi)),
\end{aligned}
\tag{2.4}
$$

where $\varphi = 2\pi/T$ denote the frequency related to the period of seasonality T and ϕ is a phase-shifting parameter to capture the timing of seasonality. The component parameters $\bar{\mu}_C$, $\bar{\mu}_L$, $\bar{\mu}_F$, $\bar{\theta}_D$, $\bar{\beta}_{LC}$, $\bar{\beta}_{CF}$ and $\bar{\beta}_{FD}$, represent the baseline rates, and a is the (relative) amplitude. Note that if $a = 0$, then there is no seasonality. A schematic representation of the model is shown in Fig. 1.

A schematic representation of the model is shown in Fig. 1.

2.2. Basic reproduction number and persistence of GWD

The reproduction number ($\mathcal{R}_0$) is a significant metric for epidemiological models as it gives insight into the potential for disease transmission. It is defined as "the expected number secondary infections generated, in a completely susceptible population, by a typical infective individual" [22]. Based on computation in Appendix A.1, the time-average reproduction number of model (2.3) is

$$\mathcal{R}_0 = \sqrt[3]{\mathcal{R}_{0LD} + \mathcal{R}_{0HD}}, \tag{2.5}$$

where

$$\mathcal{R}_{0LD} = \underbrace{\frac{p_D(1-\phi_D)\bar{\theta_D}}{\bar{\mu}_L}\left(\frac{\bar{\beta}_{FD}\gamma_D N_D}{(\gamma_D+\mu_D)(\eta_D+\mu_D)}\right)}_{\text{(i)}}\underbrace{\left(\frac{\bar{\beta}_{LC}\gamma_C N_C}{(\gamma_C+\bar{\mu}_C)\bar{\mu}_C}\right)}_{\text{(ii)}}\underbrace{\left(\frac{\bar{\beta}_{CF}N_F}{(\eta_F+\bar{\mu}_F)}\right)}_{\text{(iii)}},$$

$$\mathcal{R}_{0HD} = \underbrace{\frac{(1-p_D)\bar{\theta}_D}{\bar{\mu}_L}\left(\frac{\bar{\beta}_{FD}\gamma_D N_D}{(\gamma_D+\mu_D)(\sigma_D+\mu_D)}\right)}_{\text{(i)}}\underbrace{\left(\frac{\bar{\beta}_{LC}\gamma_C N_C}{(\gamma_C+\bar{\mu}_C)\bar{\mu}_C}\right)}_{\text{(ii)}}\underbrace{\left(\frac{\bar{\beta}_{CF}N_F}{(\eta_F+\bar{\mu}_F)}\right)}_{\text{(iii)}}.$$

The terms $\mathcal{R}_{0LD}$ and $\mathcal{R}_{0HD}$ show the contribution of lightly infected and heavily infected dogs to the generation of secondary infections. One can observe $\mathcal{R}_{0LD}$ and $\mathcal{R}_{0HD}$ are a product of three terms which describes the cycle of GW infection from dogs to larva (i), larva to copepod (ii), and copepod to fish (iii). Furthermore, we can also observe that if dogs are assumed to be of uniform mean worm burden ($p_D = \phi_D = 1$) then

$$\mathcal{R}_0 = \sqrt[3]{\underbrace{\frac{\bar{\theta}_D}{\bar{\mu}_L}\left(\frac{\bar{\beta}_{FD}\gamma_D N_D}{(\gamma_D+\mu_D)(\eta_D+\mu_D)}\right)}_{\text{(i)}}\underbrace{\left(\frac{\bar{\beta}_{LC}\gamma_C N_C}{(\gamma_C+\bar{\mu}_C)\bar{\mu}_C}\right)}_{\text{(ii)}}\underbrace{\left(\frac{\bar{\beta}_{CF}N_F}{(\eta_F+\bar{\mu}_F)}\right)}_{\text{(iii)}}}, \tag{2.6}$$

Moreover, if $p_D > 0.5$, it implies that lightly infected dogs contribute more to the generation of secondary cases compared to heavily infected dogs, and the opposite is true. Therefore, we note that understanding the role of the mean worm burden on GWD dynamics is essential for effective management of the disease. We further define the terms in $\mathcal{R}_0$ as follows: near the DFE ($\mathcal{E}^0$), the total number of dogs reaches a stable state N_D, and every dog will be susceptible. Susceptible dogs become exposed to GWD through the consumption of infectious fish at rate $\bar{\beta}_{FD}$. Exposed dogs have a probability $\frac{\gamma_D}{(\gamma_D+\mu_D)}$ to survive this state and become infectious, with a proportion p_D as lightly infected and the remainder $(1-p_D)$ as heavily infected. Lightly infected dogs discharge larvae with the density $\frac{(1-\phi_D)\bar{\theta}_D}{\bar{\mu}_L}$ per dog over its expected infectious period $\frac{1}{(\eta_D+\mu_D)}$ while heavily infected dogs discharge larvae with the density $\frac{\bar{\theta}_D}{\bar{\mu}_L}$ per dog over its expected infectious period $\frac{1}{(\sigma_D+\mu_D)}$. The total number of copepods reaches at a stable state N_C, and every copepod will be susceptible. Susceptible copepods become exposed to GWD at a rate $\bar{\beta}_{LC}$ through consumption of larvae discharge into the environment by infectious dogs. Exposed copepods have a $\frac{\gamma_C}{(\gamma_C+\bar{\mu}_C)}$ probability of surviving this state and becoming infectious throughout their entire lifespan $\frac{1}{\bar{\mu}_C}$. Additionally, the total number of fish reaches state N_F and every fish will be susceptible. Susceptible fish become infected with GWD through the consumption of infectious copepods at a rate. $\bar{\beta}_{CF}$, after which they will become infectious for a period $\frac{1}{\eta_F+\bar{\mu}_F}$.

When $\mathcal{R}_0$ is less than unity, then the GWD cannot persist, as shown in the following theorem. All the proofs are relegated to Appendix A.2.

Theorem 2.1. *If $R_0 < 1$, then the disease-free equilibrium $\mathcal{E}_0$ of system (2.3) is globally asymptotically stable.*

Suppose now $\mathcal{R}_0 > 1$. We demonstrate that the disease can persist. Let $X = \mathbb{R}^{10}_+$,

$$\begin{aligned} X_0 =& \{(E_C, I_C, I_F, E_D, I_{LD}, I_{HD}, L, S_D, S_C, S_F) \in \mathbb{R}^{10}_+ : E_C > 0, I_C > 0, I_F > 0, \\ & E_D > 0, I_{LD} > 0, I_{HD} > 0, L > 0\} \end{aligned}$$

and let $\partial X_0 = X/X_0$.

Theorem 2.2. *Let $\mathcal{R}_0 > 1$. Then system (2.3) is uniformly persistent, i.e., there exists some $\eta > 0$ such that*

$$\begin{aligned} &\liminf_{t\to\infty} S_C(t) \geq \eta, \quad \liminf_{t\to\infty} E_C(t) \geq \eta, \quad \liminf_{t\to\infty} I_C(t) \geq \eta, \quad \liminf_{t\to\infty} S_F(t) \geq \eta, \quad \liminf_{t\to\infty} I_F(t) \geq \eta, \\ &\liminf_{t\to\infty} S_D(t) \geq \eta, \quad \liminf_{t\to\infty} E_D(t) \geq \eta, \quad \liminf_{t\to\infty} I_{LD}(t) \geq \eta, \quad \liminf_{t\to\infty} I_{HD}(t) \geq \eta, \quad \liminf_{t\to\infty} L(t) \geq \eta, \end{aligned}$$

for all solutions of (2.3) with initial conditions in X_0. Moreover, (2.3) has at least one positive ω-periodic solution.

Table 1
Model parameters and their interpretations.

Symbol	Biological definition	Baseline value	Units	Source
$\frac{1}{\mu_D}$	Lifespan of dogs	10(6.8–13)	Years	[24]
$\frac{1}{\bar{\mu}_F}$	Lifespan of fish	5.5(2–5.5)	Years	[25]
$\frac{1}{\bar{\mu}_C}$	Lifespan of copepods	15.5(15.5–60)	Days	[27]
$\frac{1}{\bar{\mu}_L}$	Lifespan of larvae lifespan	7(3–7)	Days	[23]
$\frac{1}{\gamma_D}$	Duration of incubation for dogs	12(10–14)	Months	[26]
$\frac{1}{\bar{\gamma}_C}$	Duration of incubation for copepods	14(7–21)	Days	[26]
$\frac{1}{\bar{\eta}_F}$	Duration of infectious period for fish	14(7–21)	Days	[28]
$\frac{1}{\eta_D}$	Infectious period for lightly infected dogs	7(7–10)	Days	[26]
$\frac{1}{\sigma_D}$	Infectious period for heavily infected dogs	10(7–10)	Days	[26]
$\bar{\theta}_D$	Rate at which infectious dogs shed larvae	$(0.09–2.25) \times 10^6$	Months	[29]
$\bar{\beta}_{LC}$	Transmission rate from larva to copepods	$(6.6–450000) \times 10^{-6}$	Per copepod per month	[30]
$\bar{\beta}_{CF}$	Transmission rate from copepods to fish	$(0.9–4.23) \times 10^{-6}$	Per fish per month	Assumed
$\bar{\beta}_{FD}$	Transmission rate from fish to dogs	$(0.1–2.06) \times 10^{-6}$	Per dog per month	Assumed
ϕ_D	Modification factor	0.5(0–1)	Dimensionless	Assumed

3. Numerical results and discussions

3.1. Model parameterization

Due to the unavailability of data parameter values and ranges used in this study are taken from published peer-reviewed articles and are presented in Table 1. Prior studies estimate that Guinea-worm larvae live in water for 3 to 7 days [23]. In Chad, studies show that dogs have a lifespan of about 6.8 to 13 years [24]. The most common fish in Chad is *Alestes baremoze*, with a lifespan of approximately 5.5 years [25]. There is little literature on the incubation period and average infectious period of Guinea-worm disease (GWD) in dogs. However, for humans, the incubation period ranges from 10 to 14 months, and the average infectious period is about 1 week [26]. Due to the lack of information, we will use these values for our simulations, as the same type of worm affects both humans and dogs. Studies also estimate that copepods have a lifespan of around 15.5 days [27]. Research on the average infectious period of fish populations is limited. However, a few studies suggest it lasts for about 2 weeks [18,28]. Additionally, we set the population sizes to: $L = 10^6$, $S_C = 5 \times 10^6$, $E_C = 2 \times 10^6$, $I_C = 10^6$, $S_F = 8 \times 10^3$, $I_F = 2 \times 10^3$, $S_D = 2.5 \times 10^4$, $E_D = 10$, $I_{LD} = 42$ and $I_{HD} = 10$. To ensure the positivity of all the periodic functions we require $0 < a < 1$, and in all our simulations, we set $a = 0.8$ and $\phi = \pi$.

3.2. Sensitivity analysis

To determine the relative importance of each of parameter, we carry out a sensitivity analysis using the Latin hypercube sampling technique and partial rank correlation coefficients (PRCCs) [31]. The PRCCs quantify the relationship between $\mathcal{R}_0$ and individual parameters. The sign of the PRCC value indicates whether the parameter is inversely or positively correlated to the output. A model parameter with an absolute PRCC value close to unity has a significance influence on the output [31]. The output is depicted in Fig. 2. Overall, these results indicate that $\mathcal{R}_0$ increases when the following parameters are elevated: disease-transmission rates, copepod population, dog population, fish population, and the larvae shedding rate of infected dogs. In contrast, $\mathcal{R}_0$ decreases when the mortality rates of copepods and larvae, as well as the recovery rates of heavily infected dogs, are increased. Together, these findings suggest that reducing copepod population density and mitigating fish consumption by the terminal host, such as by burying fish entrails, may significantly decrease infection prevalence. Results on further inference on the relationship between $\mathcal{R}_0$ and individuals parameters are shown in Fig. 3. One can observe that reducing copepod lifespan to less than 15.5 days will reduce $\mathcal{R}_0$ below unity. This can be achieve through use of chemical

The simulation results presented in Fig. 4 illustrate the disease dynamics over time when $\mathcal{R}_0 < 1$. We initialized the populations with the following values: $L(0) = 10^6$, $S_C(0) = 5 \times 10^6$, $E_C(0) = 2 \times 10^6$, $I_C(0) = 10^6$, $S_F(0) = 8 \times 10^3$, $I_F(0) = 2 \times 10^3$, $S_D(0) = 2.5 \times 10^4$, $E_D(0) = 10$, $I_{LD}(0) = 42$ and $I_{HD}(0) = 10$. The model output indicates that all solutions converge to the disease-free equilibrium, which concurs with Theorem 2.1. We observe that even though the simulations begin with very high populations of larvae, copepods, and fish, the disease does not persist when $\mathcal{R}_0$ is less than one. Throughout all panels, we notice periodic outbreaks of the disease before it eventually becomes extinct. However, in Fig. 5, we observe that model (2.1) contains at least one positive ω-periodic solution, consistent with Theorem 2.2. It can be seen that the dynamics of the disease within the dog population will be characterized by persistent periodic outbreaks over the entire time period.

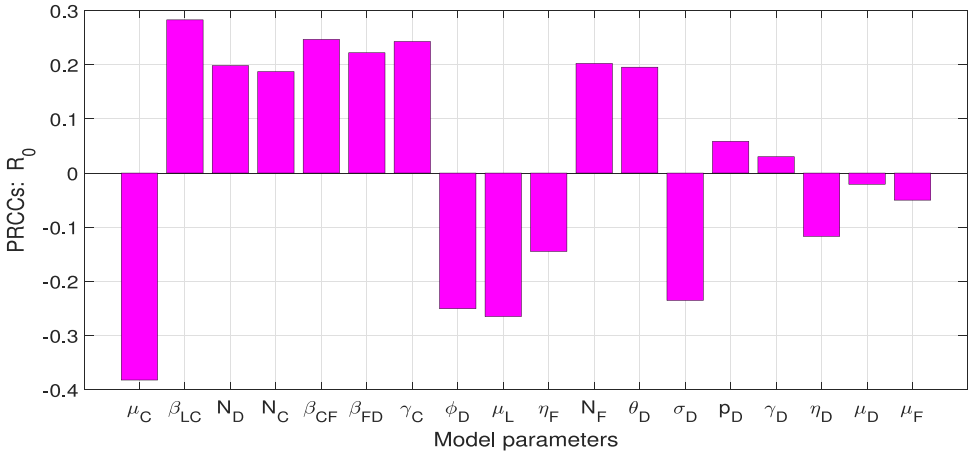

Fig. 2. Global sensitivity analysis of the reproduction number ($\mathcal{R}_0$) to key model parameters. Increasing the magnitude of the parameters μ_C, β_{LC}, β_{CF}, γ_C, μ_L and σ_D will significantly alter the size of $\mathcal{R}_0$.

3.3. Effects of mean worm burden on disease dynamics

The primary objective of this section is to examine the effects of heterogeneous mean worm burden on GWD dynamics. Thus, we simulate the model (2.3) with different values of p_D, and the results are shown in Fig. 6. As we can observe, increasing p_D increases the population of the heavily infected dog population. This in turn increases the density of larvae in the environment, since heavily infected dogs are assumed to visit water sources more frequently than lightly infected dogs. As the number of larvae in the environment increases, the population of exposed and infectious copepods increases. However, we can observe that an increase in p_D does not significantly change the infectious fish population or the exposed dog population. Overall, we can conclude that increasing p_D increases the potential for disease transmission.

3.4. Effects of dog-intervention strategies on disease dynamics

Since the discovery of GW infections in dogs, responsible authorities have been encouraging communities and offering rewards to individuals who report and tether their infected dog [32]. This technique is also credited with the current decline in GW infections in dogs. Therefore, it is essential to evaluate the effects of dog screening on disease dynamics. Since dog screening increases the rate of recovery of dog populations, we rewrite $\eta_D = \eta_{D0} + u_D$ and $\sigma_D = \sigma_{D0} + u_D$, where u_D represent dog screening and η_{D0} and σ_{D0} denote the recovery of lightly infected and heavily infected dogs, respectively, in the absence of screening. Following the approach in [19], let the monthly percentage of dog detected be $C_D = 100[1 - e^{-u_D}]$. Consequently, the exit rate from the light and heavily infected compartments, respectively, is

$$\eta_D = \eta_{D0} - \ln\left(1 - \frac{C_D}{100}\right) \quad \text{and} \quad \sigma_D = \sigma_{D0} - \ln\left(1 - \frac{C_D}{100}\right). \tag{3.1}$$

Simulating model (2.3) for different values of C_D yields results in Fig. 7. As we can observe, increasing dog screening will significantly reduce exposed and infectious copepod population, infectious dog population and larvae density in the environment. However, it is worth noting that even at 90% detection, dog screening alone may not sufficiently lead to the eradication of GWD.

4. Concluding remarks

Seasonal fluctuations are a common characteristic of many infectious diseases, and a recent study on Guinea-worm disease (GWD) datasets for dog infection in Chad has identified seasonal patterns in the disease dynamics [8]. Additionally, field studies have revealed that the mean worm burden in infected dogs is heterogeneous, with some dogs harboring significantly more parasites than others [6]. These observations motivated the development of a non-autonomous model of the Guinea-worm lifecycle, which takes into account the complexities of the disease transmission cycle. The model specifically focuses on dogs as the sole terminal host, with copepods and fish serving as intermediate hosts. By considering these factors, the model aims to provide a more nuanced understanding of GWD dynamics and inform the development of effective control strategies.

To account for the variability in worm burden among infected dogs, we subdivided the infectious dog population into two groups: lightly infected and heavily infected dogs. To capture the impacts of seasonal fluctuations on disease dynamics, we employed time-dependent functions to model the recruitment and mortality rates of fish, copepods, disease transmission rates, and the rate at which infectious dogs shed larvae into the environment, as well as the lifespan of larvae in the environment. Using our model, we computed the reproduction number and performed a sensitivity analysis. The results revealed that increasing the mortality rate of copepods

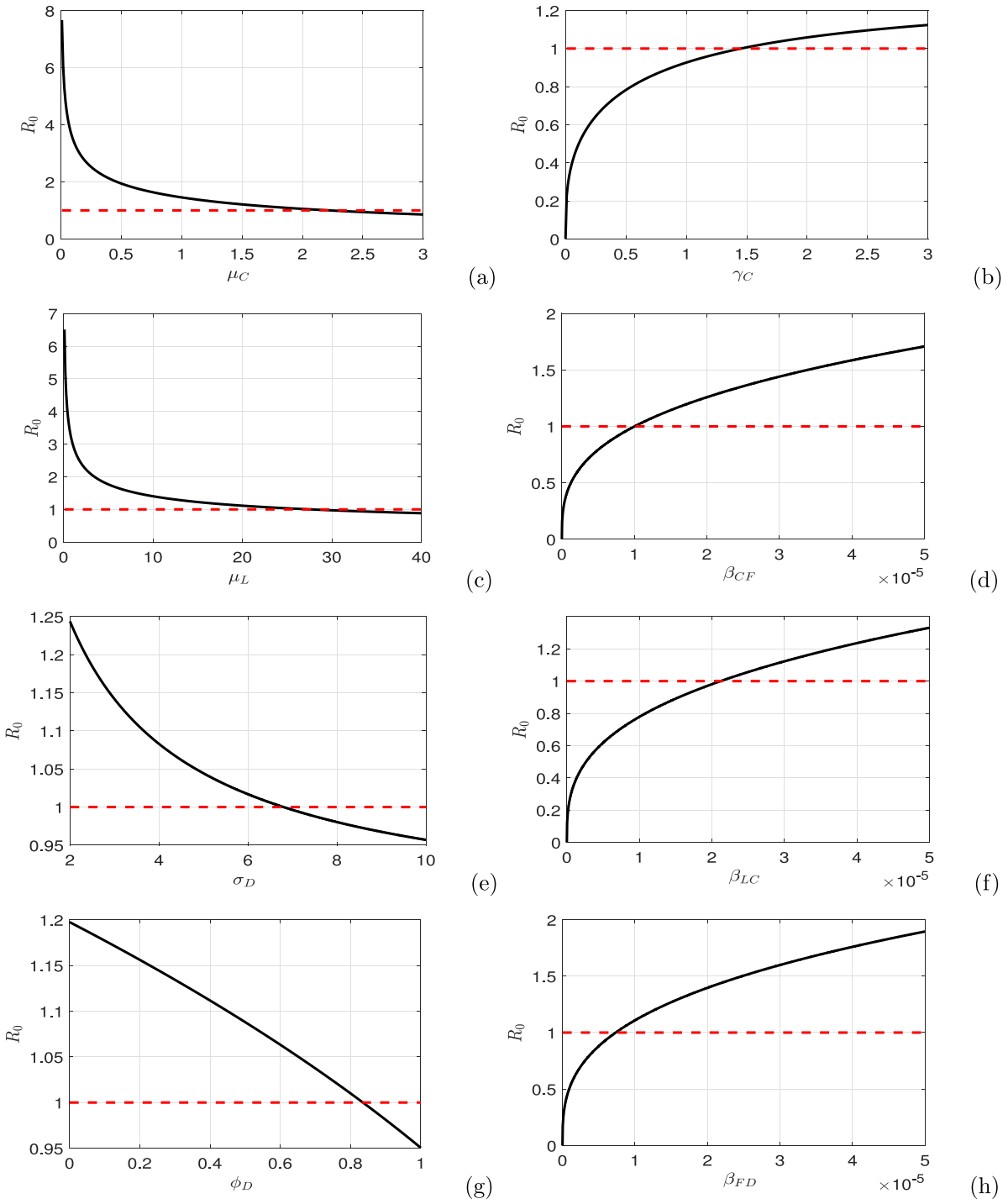

Fig. 3. Simulation results showing the relationship between $\mathcal{R}_0$ and individuals parameters. One can observe that when any of the parameters in the left panel ((a), (c), (e), (g)) are increased $\mathcal{R}_0$ decreases. In contrast, increasing parameters in the right panel ((b), (d), (f), (h)) are increased $\mathcal{R}_0$ increases.

significantly decreases the reproduction number, suggesting a potential route to controlling the disease. In particular, we observed that whenever the lifespan of copepods is reduced to less than 15 days then the reproduction number will be always less than unity. These results are consistent with the findings of existing literature [12,13,18]. Although reduction of copepod population can be achieved through the use of Abate, it is worth noting that, during the rainy season, there will be several water pools containing paratenic hosts. As a result, the success of this intervention strategy will be somewhat limited.

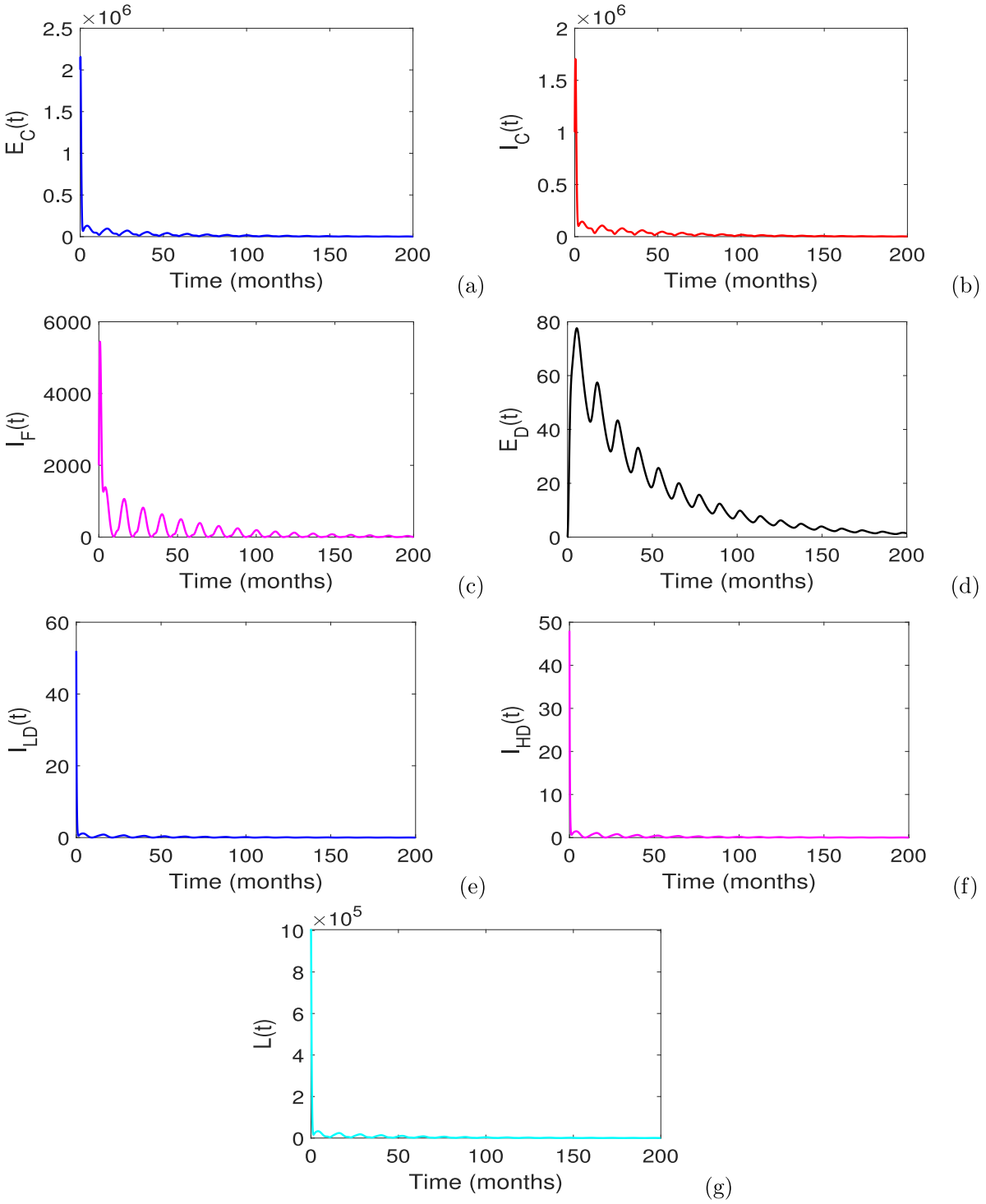

Fig. 4. Simulation results showing disease dynamics when $\mathcal{R}_0 = 0.937 < 1$. Baseline parameters are given in Table 1. We can observe that all solutions converge to the disease-free equilibrium and this is in agreement to Theorem 2.1.

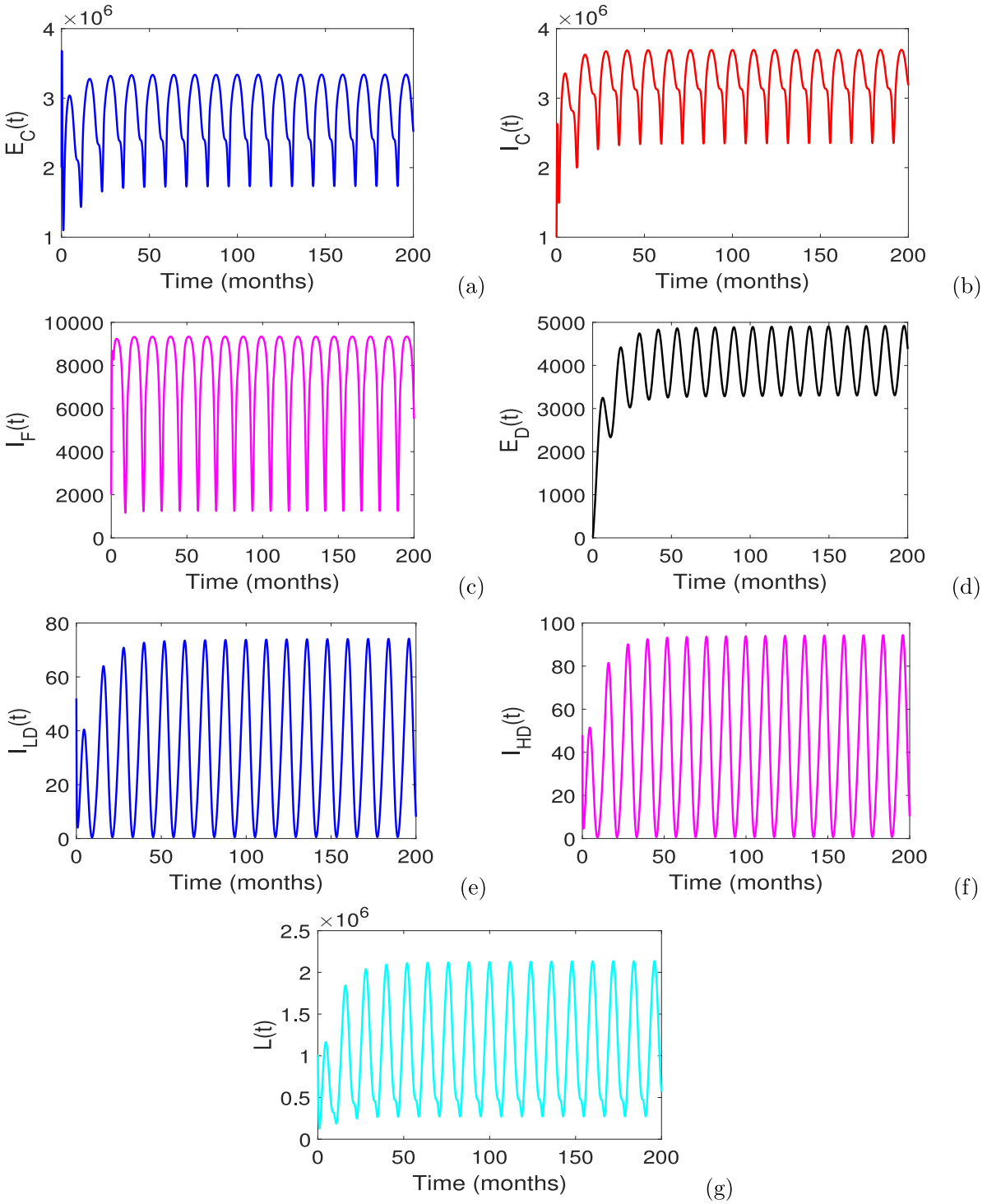

Fig. 5. Simulation results showing disease dynamics when $\mathcal{R}_0 = 6.7753 > 1$. Baseline parameters are given in Table 1. One can observe that model (2.3) has at least one positive ω-periodic solution and this is in agreement to Theorem 2.2.

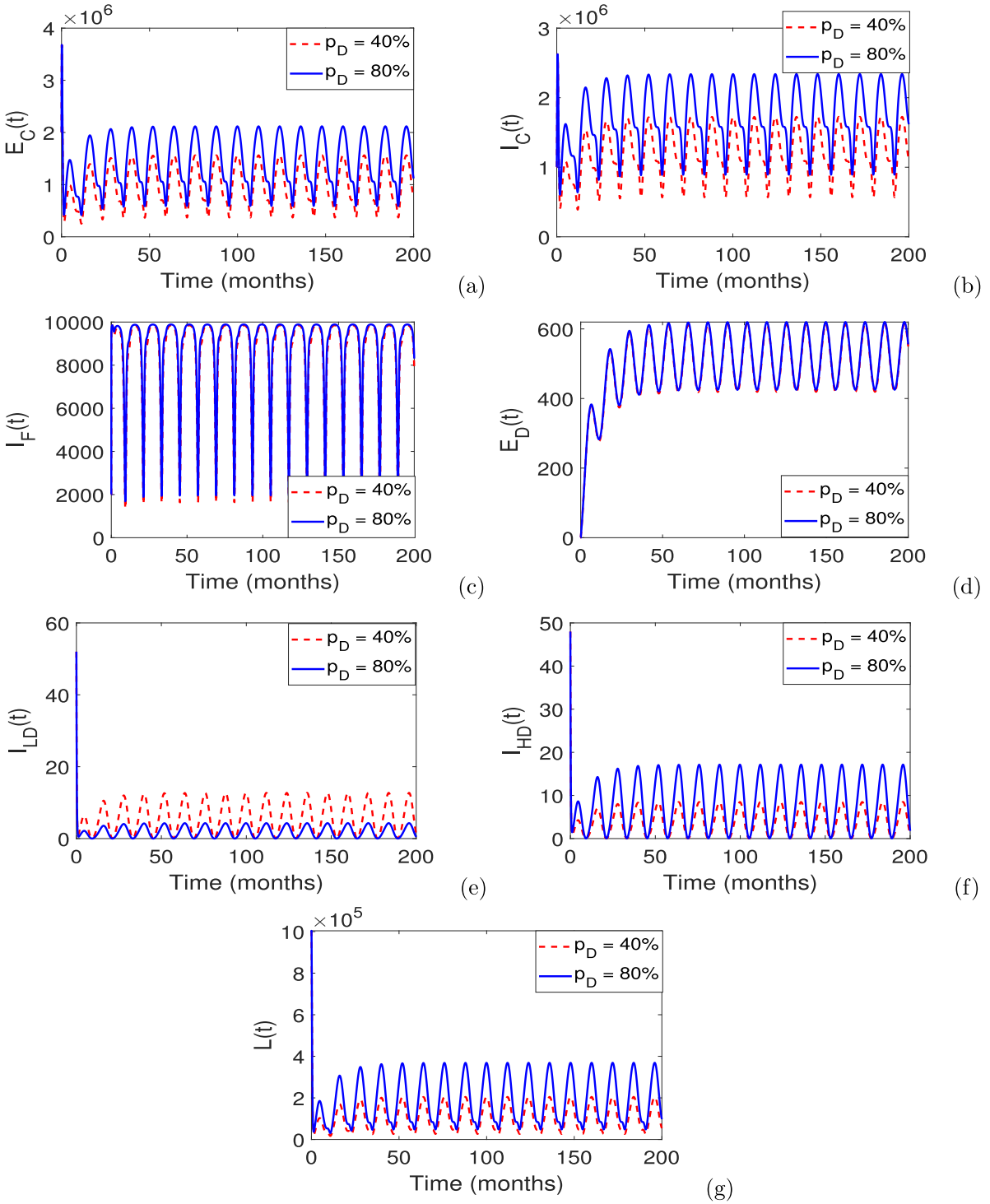

Fig. 6. Simulation results capture the impact of mean worm burden on disease dynamics over a period of 200 months. In panels (a)–(g), the results compare the effects of 40% and 80% of infectious dogs being lightly infected.

We also observed that increasing the detection rate of heavily infected dogs can reduce the reproduction number, although this effect was less pronounced compared to the impact of copepod mortality rate. Our findings collectively suggest that augmenting copepod mortality rates and reducing the rate at which dogs consume fish could synergistically reduce infection prevalence.

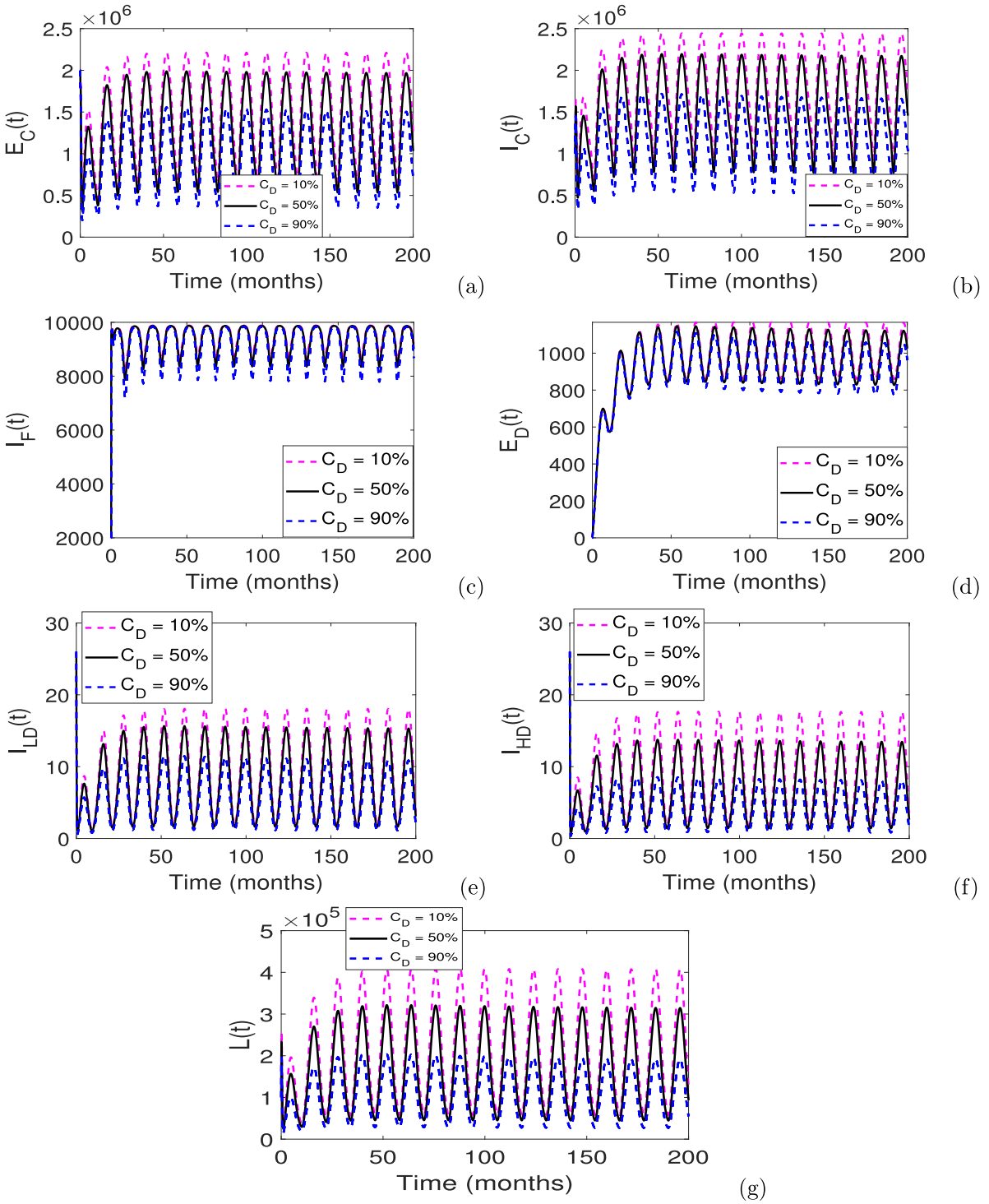

Fig. 7. Simulation results illustrate the impact of dog screening on disease dynamics. In general, it is evident that higher screening rates lead to a decrease in the number of infected populations. However, it is worth noting that even with a 90% success rate, this approach alone may not be enough to eliminate GWD.

These insights underscore the value of targeted interventions aimed at controlling key ecological and biological factors driving the transmission of Guinea Worm Disease.

Our numerical analysis examined the effect of varied mean worm burden on disease dynamics. The results indicated that an increase in heavily infected dogs significantly raises infection rates in both copepods and dogs. However, the fish population remains mostly unaffected. Notably, our findings show that even with a 90% detection rate, screening dogs alone may not be enough to eliminate Guinea Worm Disease (GWD). This implies that detection efforts may not suffice to eradicate GW infections in dog populations. Therefore, our model suggests a more effective eradication strategy. This strategy would combine detecting and restraining infectious dogs with efforts to reduce their fish consumption, such as burying fish entrails as proposed by Engelhard et al. [18]. By implementing a multi-faceted approach that addresses both detection and prevention of disease transmission, we may succeed in eradicating GWD.

Additionally, the model highlights that the presence of heterogeneous mean worm burdens in the dog population poses a significant challenge to guinea worm control. We note that the increase in recovery rate of heavily infected dogs significantly reduces the disease transmission potential. In particular, we observed that when e heavily infected dog takes more than 5 days to recover, the disease persists in the community. This happens because the reproduction number remain greater than one. Therefore, we can conclude that a multi-faceted approach is essential for effectively controlling the disease.

Model limitations and future directions

Despite these findings, our model has limitations. First, we recommend expansion of this work through calibration of the proposed model with data from GWD endemic settings while inferring parameter uncertainty. The availability of such data will be crucial in determining appropriate mathematical functions capable of capturing seasonal variability in GW infections.

Second, in this study we considered fish as the only source of GWD infection for dogs. However, other researchers indicate that dogs can also get infected by eating frogs and tadpoles [17]. While it is quite possible to reduce dog consumption of fish entrails through educational campaigns about burial, it may be harder to limit dogs eating frogs and tadpoles. These amphibians are often plentiful in shallow water during the rainy season, making them easy for FRDs to access. Including these secondary hosts in our model is essential for accurately estimating the transmission intensities needed to eliminate GWD.

Third, the transmission potential of GWD is affected by how mobile dogs are. In countries where GWD is common, many dogs are FRDs. This highlights the need for future research to include reaction–diffusion equations. Such equations will help us understand local transmission dynamics and the movement of dogs, which is vital for controlling the disease. Furthermore, the non-autonomous model in this study has limitations in capturing GWD complexities. It does not fully address uncertainty in disease transmission. Future research should focus on stochastic modeling to fill these gaps. Stochastic models can account for uncertainty in disease spread, allowing researchers to estimate the chances of an outbreak or disease extinction when a single host enters a community. Given the low number of reported human cases, stochastic models are particularly useful for predicting the disease's extinction and persistence. Additionally, by incorporating uncertainty and variability, these models can provide valuable insights for policymakers and public-health officials, helping them make informed decisions about GWD.

CRediT authorship contribution statement

Eva Lusekelo: Formal analysis, Conceptualization. **Salamida Daudi:** Methodology, Formal analysis. **Mlyashimbi Helikumi:** Writing – original draft, Methodology. **Steady Mushayabasa:** Writing – review & editing, Supervision.

Declaration of Generative AI and AI-assisted technologies in the writing process

During the preparation of this work the authors utilized AI to improve language and readability. After using this tool, the authors reviewed and edited the content as needed and take full responsibility for the content of the publication.

Funding

No funding was received to carry out this study.

Declaration of competing interest

The authors declare that they have no known competing financial or personal relationships that could have appeared to influence the work reported in this study.

Acknowledgments

Authors are grateful to two anonymous reviewers for their invaluable comments and suggestions, which greatly improved the presentation of this paper. The views, opinions, assumptions or any other information expressed in this article are solely those of the authors.

Appendix A. Dynamical analysis of the proposed model

A.1. Basic reproduction number

To compute $\mathcal{R}_0$, one commences by establishing the disease-free equilibrium (DFE). For model (2.3) one can easily verify that, in the absence of the disease, the system admits a disease-free periodic model $\mathcal{E}^0 = (N_C, 0, 0, N_F, 0, N_D, 0, 0, 0, 0, 0)$. Linearizing model (2.3) at $\mathcal{E}^0$ leads to the following system for infected compartments

$$\begin{aligned}
E_c'(t) &= \beta_{LC}(t)N_C - (\mu_C(t) + \gamma_C)E_C,\\
I_c'(t) &= \gamma_C E_C - \mu_C(t)I_C,\\
I_F'(t) &= \beta_{CF}(t)I_C N_F - (\mu_F(t) + \eta_F)I_F,\\
E_D'(t) &= \beta_{FD}(t)I_F N_D - (\mu_D + \gamma_D)E_D,\\
I_{LD}'(t) &= p_D\gamma_D E_D - (\mu_D + \eta_D)I_D,\\
I_{HD}'(t) &= (1-p_D)\gamma_D E_D(t) - (\mu_D + \sigma_D)I_{HD},\\
L'(t) &= \theta_D(t)(1-\phi_D)I_{LD} + \theta_D(t)I_{HD} - \mu_L(t)L.
\end{aligned} \tag{A.1}$$

We can write linear system (A.1) as

$$\frac{du}{dt} = [F(t) - V(t)]u(t), \tag{A.2}$$

for all $t \geq 0$, where $u(t)$ is a column vector of variables representing infected compartments; i.e., $u(t) = (E_C(t), I_C(t), I_F(t), E_D(t), I_{LD}(t), I_{HD}(t))$. $F(t)$ and $V(t)$ are given by

$$F(t) = \begin{bmatrix}
0 & 0 & 0 & 0 & 0 & 0 & \beta_{LC}(t)N_C\\
0 & 0 & 0 & 0 & 0 & 0 & 0\\
0 & \beta_{CF}(t)N_F & 0 & 0 & 0 & 0 & 0\\
0 & 0 & \beta_{FD}(t)N_D & 0 & 0 & 0 & 0\\
0 & 0 & 0 & 0 & 0 & 0 & 0\\
0 & 0 & 0 & 0 & 0 & 0 & 0\\
0 & 0 & 0 & 0 & 0 & 0 & 0
\end{bmatrix}, \tag{A.3}$$

and

$$V(t) = \begin{bmatrix}
\mu_C(t) + \gamma_C & 0 & 0 & 0 & 0 & 0 & 0\\
-\gamma_C & \mu_C(t) & 0 & 0 & 0 & 0 & 0\\
0 & 0 & \mu_C(t) + \eta_F & 0 & 0 & 0 & 0\\
0 & 0 & 0 & \mu_D + \gamma_D & 0 & 0 & 0\\
0 & 0 & 0 & -p_D\gamma_D & \mu_D + \eta_D & 0 & 0\\
0 & 0 & 0 & -(1-p_D)\gamma_D & 0 & \mu_D + \sigma_D & 0\\
0 & 0 & 0 & 0 & \theta_D(t)(1-\phi_D) & \theta_D(t) & \mu_L(t)
\end{bmatrix}. \tag{A.4}$$

Let $\Phi_V(t)$ and $\rho(\Phi_V(\omega))$ be the monodromy matrix of the linear ω-periodic system $u_t = V(t)u$ and the spectral radius of $\Phi_V(\omega)$, respectively. Let $Y(t,s)$, $t \geq s$, be the evolution of the linear periodic system $\frac{dy}{dt} = V(t)y$. That is, for each $s \in \mathbb{R}$, the 7×7 matrix $Y(t,s)$ satisfies

$$\frac{d}{dt}Y(t,s) = V(t)Y(t,s), \qquad \forall t \geq s, \qquad Y(s,s) = I,$$

where I is the 7×7 identity matrix.

Let C_ω be the ordered Banach space of all $\omega-$periodic functions from $\mathbb{R}$ to $\mathbb{R}^7$, equipped with the maximum norm $\|\cdot\|$ and the positive cone $C_\omega^+ := \{\phi(t) \geq 0, \forall t \in \mathbb{R}\}$. It follows from Wang and Zhao (2008) [33] that $\phi(s) \in C_\omega$ represents the initial distribution of infectious host and vector. Then $F(s)\phi(s)$ is the distribution of new infections generated by the infectious larvae, intermediate and definitive host who were introduced at time s and remain in the infectious compartment at time t. It follows that

$$\psi(t) \equiv \int_{-\infty}^{t} Y(t,s)F(s)\phi(s)ds = \int_0^{\infty} Y(t,t-a)F(t-a)\phi(t-a)da,$$

is the distribution of cumulative infections at time t produced by L1 larvae, intermediate and definitive host $\phi(s)$ introduced at previous time to t.

Let a linear operator $\mathcal{L} : C_\omega \to C_\omega$ be defined by

$$(\tilde{L}\phi)(t) = \int_0^{\infty} Y(t,t-a)F(t-a)\phi(t-a)da, \qquad \forall t \in \mathbb{R}, \qquad \phi \in C_\omega.$$

The operator $\mathcal{L}$ can be called the next-infection operator, and its spectral radius $\rho(\mathcal{L})$ can be defined as the basic reproduction number for system (2.3)

$$R_0 = \rho(\mathcal{L}). \tag{A.5}$$

In order to estimate $\mathcal{R}_0$ in the periodic case, following Wang and Zhao (2008) [33], we let $U(t,\lambda)$ be the monodromy matrix of the following linear-periodic system

$$\frac{dU}{dt} = \left(\frac{F(t)}{\lambda} - V(t)\right)U(t),$$

with parameter $\lambda \in (0,\infty)$. Thus, we have the following results.

Lemma A.1 (*Theorem 2.1 in Wang and Zhao [33]*)**.** *The following statements are valid.*
(i) *If* $\rho(U(\omega,\lambda)) = 1$ *has a positive root* λ_0*, then* λ_0 *is an eigenvalue of* $\mathcal{L}$*, and hence* $\mathcal{R}_0 = 0$.
(ii) *If* $R_0 > 0$*, then* $\lambda = R_0$ *is the unique root of* $\rho(U(\omega,\lambda)) = 1$.
(iii) $R_0 = 0$ *if and only if* $\rho(U(\omega,\lambda)) < 1$ *for all* $\lambda > 0$.

It follows from Lemma A.1 that $\mathcal{R}_0$ is the unique solution of $\rho(U(\omega,\lambda)) = 1$. The basic reproduction number in Eq. (A.5) can be numerically evaluated by utilizing the method described in [34]. On the local asymptotic stability of the disease-free periodic solution, the following results can be deduced from Theorem 2.2 in Wang and Zhao [33].

Lemma A.2 (*Theorem 2.2 in Wang and Zhao [33]*)**.** *The following statements are valid:*
(i) $\mathcal{R}_0 = 1$*, if and only if* $\rho(\Phi_{F-V}(\omega)) = 1$;
(ii) $\mathcal{R}_0 > 1$*, if and only if* $\rho(\Phi_{F-V}(\omega)) > 1$;
(iii) $\mathcal{R}_0 < 1$*, if and only if* $\rho(\Phi_{F-V}(\omega)) < 1$.

Therefore, we can conclude that $\mathcal{E}^0$ is locally asymptotically stable if $\mathcal{R}_0 < 1$ and unstable if $\mathcal{R}_0 > 1$, where $\Phi_{F-V(t)}(\omega)$ is the monodromy matrix of the linear periodic system (2.3). Furthermore, by closely following the next-generation-matrix approach presented in [35], one can easily verify that the time-average reproduction number of model (2.3) is

$$\mathcal{R}_0 = \sqrt[3]{\mathcal{R}_{0LD} + \mathcal{R}_{0HD}}, \tag{A.6}$$

where

$$\mathcal{R}_{0LD} = \frac{p_D(1-\phi_D)\bar{\theta}_D}{\bar{\mu}_L}\left(\frac{\bar{\beta}_{FD}\gamma_D N_D}{(\gamma_D+\mu_D)(\eta_D+\mu_D)}\right)\left(\frac{\bar{\beta}_{LC}\gamma_C N_C}{(\gamma_C+\bar{\mu}_C)\bar{\mu}_C}\right)\left(\frac{\bar{\beta}_{CF}N_F}{(\eta_F+\bar{\mu}_F)}\right),$$
$$\mathcal{R}_{0HD} = \frac{(1-p_D)\bar{\theta}_D}{\bar{\mu}_L}\left(\frac{\bar{\beta}_{FD}\gamma_D N_D}{(\gamma_D+\mu_D)(\sigma_D+\mu_D)}\right)\left(\frac{\bar{\beta}_{LC}\gamma_C N_C}{(\gamma_C+\bar{\mu}_C)\bar{\mu}_C}\right)\left(\frac{\bar{\beta}_{CF}N_F}{(\eta_F+\bar{\mu}_F)}\right).$$

The terms $\mathcal{R}_{0LD}$ and $\mathcal{R}_{0HD}$ show the contribution of lightly infected and heavily infected dogs to the generation of secondary infections.

A.2. Global stability of the disease-free equilibrium

In this section, we aim to study the global dynamics of the disease-free equilibrium $\mathcal{E}^0$. From the second, fifth and seventh equations of system (2.1) one can easily verify that

$$S_C'(t) \le \mu_C(t)N_C - \mu_C(t)S_C, \quad S_F'(t) \le \mu_F(t)N_F - \mu_F(t)S_F, \quad S_D'(t) \le \mu_D N_D - \mu_D S_D. \tag{A.7}$$

Recall that any nonnegative solution $(S_C(t),\ S_F(t),\ S_D(t))$ of model (2.3) approaches $(N_C,\ N_F,\ N_D)$ as $t \to \infty$. Utilizing the standard comparison theorem (see, e.g., [36, Theorem A.4]), it follows that for any $\epsilon > 0$, there is a $T > 0$ such that:

$$S_C(t) < N_C + \epsilon, \qquad S_F(t) < N_F + \epsilon, \qquad S_D(t) < N_D + \epsilon, \text{ for } t > T. \tag{A.8}$$

Thus, for $t > T$, we have

$$\begin{aligned}
E_C'(t) &\le \beta_{LC}(t)L(N_C+\epsilon) - (\mu_C(t)+\gamma_C)E_C,\\
I_c'(t) &\le \gamma_C E_C - \mu_C(t)I_C,\\
I_F'(t) &\le \beta_{CF}(t)I_C(N_F+\epsilon) - (\mu_F(t)+\eta_F)I_F,\\
E_D'(t) &\le \beta_{FD}(t)I_F(N_D+\epsilon) - (\mu_D+\gamma_D)E_D,\\
I_{LD}'(t) &\le p_D\gamma_D E_D - (\mu_D+\eta_D)I_D,\\
I_{HD}'(t) &\le (1-p_D)\gamma_D E_D - (\mu_D+\sigma_D)I_{HD},\\
L'(t) &\le \theta_D(t)(1-\phi_D)I_{LD} + \theta_D(t)I_{HD} - \mu_L(t)L.
\end{aligned} \tag{A.9}$$

Define

$$F_\epsilon(t) = \begin{bmatrix} 0 & 0 & 0 & 0 & 0 & 0 & \beta_{LC}(t)(N_C+\epsilon) \\ 0 & 0 & 0 & 0 & 0 & 0 & 0 \\ 0 & \beta_{CF}(t)(N_F+\epsilon) & 0 & 0 & 0 & 0 & 0 \\ 0 & 0 & \beta_{FD}(t)(N_D+\epsilon) & 0 & 0 & 0 & 0 \\ 0 & 0 & 0 & 0 & 0 & 0 & 0 \\ 0 & 0 & 0 & 0 & 0 & 0 & 0 \\ 0 & 0 & 0 & 0 & 0 & 0 & 0 \end{bmatrix}.$$

By [33, Theorem 2.2], we have $R_0 < 1 \iff \rho(\phi_{F-V}(\omega)) < 1$, where $\rho(\phi_{F-V}(\omega))$ is the spectral radius of $\phi_{F-V}(\omega)$ and $\phi_{F-V}(\omega)$ is the monodromy matrix of the linear ω-periodic system $dy/dt = (F-V)y$. Then we can set ϵ sufficiently small such that $\rho(\phi_{F_\epsilon - V}(\omega)) < 1$. Consequently, the trivial solution $(0,0,0,0,0,0,0)$ of the following linear ω-periodic system

$$\begin{aligned} E_c'(t) &= \beta_{LC}(t)L(N_C+\epsilon) - (\mu_C(t)+\gamma_C)E_C, \\ I_c'(t) &= \gamma_C E_C - \mu_C(t)I_C, \\ I_F'(t) &= \beta_{CF}(t)I_C(N_F+\epsilon) - (\mu_F(t)+\eta_F)I_F, \\ E_D'(t) &= \beta_{FD}(t)I_F(N_D+\epsilon) - (\mu_D+\gamma_D)E_D, \\ I_{LD}'(t) &= p_D\gamma_D E_D - (\mu_D+\eta_D)I_D, \\ I_{HD}'(t) &= (1-p_D)\gamma_D E_D - (\mu_D+\sigma_D)I_{HD}, \\ L'(t) &= \theta_D(t)(1-\phi_D)I_{LD} + \theta_D(t)I_{HD} - \mu_L(t)L, \end{aligned} \tag{A.10}$$

is globally asymptotically stable. Once again, making use of the comparison theorem leads to $E_C(t) \to 0$, $I_C(t) \to 0$, $I_F(t) \to 0$, $E_D(t) \to 0$, $I_{LD}(t) \to 0$, $I_{HD}(t) \to 0$ as $t \to \infty$ for $i = 1, 2$. Finally, the second, fifth and seventh equations of system (2.3) imply that $S_C(t) \to S_C^0(t)$, $S_F(t) \to S_F^0(t)$ and $S_D(t) \to S_D^0$ as $t \to \infty$. This completes the proof.

A.3. Existence of positive periodic solutions

Our main concern in the present section will be to investigate the dynamics of the system (2.3) whenever $\mathcal{R}_0 > 1$. In particular, we will demonstrate that if $\mathcal{R}_0 > 1$, the GW infection persists and there exists a positive periodic solution. By closely following the approach in [37], we define

$$X = \mathbb{R}_+^{10}; \qquad X_0 = \mathbb{R}_+^3 \times \mathrm{Int}(\mathbb{R}_+)^7; \qquad \partial X_0 = X \backslash X_0.$$

Let $P : X \longrightarrow X$ be the Poincaré map associated with our system (2.3) such that $P(x_0) = u(\omega, x_0)\ \forall x_0 \in X$, where $u(t, x_0)$ denotes the unique solution of the system with $u(0, x_0) = x_0$.

Definition A.1. The solutions of system (2.3) are said to be uniformly persistent if there exists some $\eta > 0$ such that

$$\begin{aligned} &\liminf_{t\to\infty} S_C(t) \geq \eta, \quad \liminf_{t\to\infty} E_C(t) \geq \eta, \quad \liminf_{t\to\infty} I_C(t) \geq \eta, \quad \liminf_{t\to\infty} S_F(t) \geq \eta, \quad \liminf_{t\to\infty} I_F(t) \geq \eta, \\ &\liminf_{t\to\infty} S_D(t) \geq \eta, \quad \liminf_{t\to\infty} E_D(t) \geq \eta, \quad \liminf_{t\to\infty} I_{LD}(t) \geq \eta, \quad \liminf_{t\to\infty} I_{HD}(t) \geq \eta, \quad \liminf_{t\to\infty} L(t) \geq \eta, \end{aligned}$$

whenever $S_C(0) > 0$, $E_C(0) > 0$, $I_C(0) > 0$, $S_F(0) > 0$, $I_F(0) > 0$, $S_D(0) > 0$, $E_D(0) > 0$, $I_{LD}(0) > 0$, $I_{HD}(0) > 0$, $L(0) > 0$.

Let us define

$$\begin{aligned} M_\partial = \{&(S_C(0), E_C(0), I_C(0), S_F(0), I_F(0), S_D(0), E_D(0), I_{LD}(0), I_{HD}(0), L(0)) \\ &\in \partial X_0 : P^m(S_C(0), E_C(0), I_C(0), S_F(0), I_F(0), S_D(0), E_D(0), I_{LD}(0), I_{HD}(0), L(0)) \\ &\in \partial X_0, \forall m \geq 0\}, \end{aligned}$$

and

$$\widetilde{M}_\partial = \{(S_C(0), S_D(0), S_F(0), 0, 0, 0, 0, 0, 0, 0) : S_C \geq 0, S_F \geq 0, S_D \geq 0\}. \tag{A.11}$$

We first show that

$$M_\partial = \widetilde{M}_\partial. \tag{A.12}$$

It follows that $M_\partial \supseteq \widetilde{M}_\partial$. Consider any initial values $(S_C(0), E_C(0), I_C(0), S_F(0), I_F(0), S_D(0), E_D(0), I_{LD}(0), I_{HD}(0), L(0)) \in \partial X_0 \backslash \widetilde{M}_\partial$. If $E_C(0) = I_C(0) = I_F(0) = 0$, $E_D(0) = I_{LD}(0) = I_{HD}(0) = 0$ and $L(0) > 0$, we have $E_C'(0) > 0$. In a similar manner, one can easily demonstrate that $I_F'(0) > 0$, $E_D'(0) > 0$ $I_{LD}'(0) > I_{HD}'(0) > 0$ and $L'(0) > 0$. Therefore, it follows that $(S_C(t), E_C(t), I_C(t), S_F(t), I_F(t), S_D(t), E_D(t), I_{LD}(t), I_{HD}(t), L(t)) \notin \partial X_0$ for $0 < t \ll 1$. The positive invariance of X_0 implies that $M_\partial = \widetilde{M}_\partial$; hence, Eq. (A.12) holds.

Now, let us consider the fixed point $M_0 = \left(S_C^0(t), 0, 0, S_F^0(t), 0, S_D^0, 0, 0, 0, 0\right)$ and define $W^S(M_0) = \{x_0 : P^m(x_0) \to M_0, m \to \infty\}$. From system (2.3), one can deduce that when $E_C = I_C = I_F = E_D = I_{LD} = I_{HD} = L = 0$, we have $S_C(t) \to S_C^0(t)$, $S_F(t) \to S_F^0(t)$, $S_D(t) \to S_D^0$ as $t \to \infty$. We demonstrate that

$$W^S(M_0) \cap X_0 = \emptyset. \tag{A.13}$$

Let $\|\cdot\|$ denote a norm on $\mathbb{R}_+^{10}$. Since all solutions of system (2.3) are continuous with respect to initial conditions, it follows that for any $\epsilon > 0$, there exists $\delta > 0$ small enough such that for all $(S_C(0), E_C(0), I_C(0), S_F(0), I_F(0), S_D(0), E_D(0), I_{LD}(0), I_{HD}(0), L(0)) \in X_0$ with $\| (S_C(0), E_C(0), I_C(0), S_F(0), I_F(0), S_D(0), E_D(0), I_{LD}(0), I_{HD}(0), L(0)) - M_0 \| \leq \delta$, this gives

$$\begin{aligned} &\|u(t, (S_C(0), E_C(0), I_C(0), S_F(0), I_F(0), S_D(0), E_D(0), I_{LD}(0), I_{HD}(0), L(0))) - u(t, M_0)\| < \epsilon, \\ &\forall\ t \in [0, \omega]. \end{aligned} \tag{A.14}$$

We claim that

$$\begin{aligned} &\limsup_{m\to\infty} \|P^m(S_C(0), E_C(0), I_C(0), S_F(0), I_F(0), S_D(0), E_D(0), I_{LD}(0), I_{HD}(0), L(0)) - M_0\| \geq \delta, \\ &\forall\ (S_C(0), E_C(0), I_C(0), S_F(0), I_F(0), S_D(0), E_D(0), I_{LD}(0), I_{HD}(0), L(0)) \in X_0. \end{aligned} \tag{A.15}$$

One can demonstrate this claim by contradiction. Suppose

$$\limsup_{m\to\infty} \|P^m(S_C(0), E_C(0), I_C(0), S_F(0), I_F(0), S_D(0), E_D(0), I_{LD}(0), I_{HD}(0), L(0)) - M_0\| < \delta, \tag{A.16}$$

for some $(S_C(0), E_C(0), I_C(0), S_F(0), I_F(0), S_D(0), E_D(0), I_{LD}(0), I_{HD}(0), L(0)) \in X_0$. Without loss of generality, we assume that

$$\|P^m(S_C(0), E_C(0), I_C(0), S_F(0), I_F(0), S_D(0), E_D(0), I_{LD}(0), I_{HD}(0), L(0)) - M_0\| < \delta, \quad \forall m \geq 0. \tag{A.17}$$

Thus,

$$\begin{aligned} &\|u(t, P^m(S_C(0), E_C(0), I_C(0), S_F(0), I_F(0), S_D(0), E_D(0), I_{LD}(0), I_{HD}(0), L(0))) - u(t, M_0)\| < \epsilon, \\ &\forall\ t \in [0, \omega], \quad m \geq 0. \end{aligned} \tag{A.18}$$

Moreover, for any $t \geq 0$, we can write $t = t' + n\omega$ with $t' \in [0, \omega]$ and n being the greatest integer less than or equal to t/ω. Then we get

$$\begin{aligned} &\|u(t, (S_C(0), E_C(0), I_C(0), S_F(0), I_F(0), S_D(0), E_D(0), I_{LD}(0), I_{HD}(0), L(0))) - u(t, M_0)\| \\ &= \|u(t', P^m(S_C(0), E_C(0), I_C(0), S_F(0), I_F(0), S_D(0), E_D(0), I_{LD}(0), I_{HD}(0), L(0))) - u(t', M_0)\| < \epsilon, \end{aligned} \tag{A.19}$$

for any $t \geq 0$. Let

$$\begin{aligned} &(S_C(t), E_C(t), I_C(t), S_F(t), I_F(t), S_D(t), E_D(t), I_{LD}(t), I_{HD}(t), L(t)) \\ &= u(t, (S_C(0), E_C(0), I_C(0), S_F(0), I_F(0), S_D(0), E_D(0), I_{LD}(0), I_{HD}(0), L(0))). \end{aligned} \tag{A.20}$$

It follows that

$$\begin{aligned} &S_C^0(t) - \epsilon < S_C(t) < S_C^0(t) + \epsilon, \quad S_F^0(t) - \epsilon < S_F(t) < S_F^0(t) + \epsilon, \quad S_D^0 - \epsilon < S_D(t) < S^0 D + \epsilon, \\ &0 < E_C(t) < \epsilon, \quad 0 < I_C(t) < \epsilon, \quad 0 < I_F(t) < \epsilon, 0 < E_D(t) < \epsilon, \quad 0 < I_{LD}(t) < \epsilon, \quad 0 < I_{HD}(t) < \epsilon, \\ &0 < I_{HD}(t) < \epsilon. \end{aligned}$$

Thus

$$\begin{aligned} \frac{dE_C}{dt} &= \beta_{LC}(t) L S_C - (\mu_C(t) + \gamma_C) E_C \\ &\geq \beta_{LC}(t) L (N_C - \epsilon) - (\mu_C(t) + \gamma_C) E_C \\ &= -(\mu_C(t) + \gamma_C) E_C + \beta_{LC}(t) L N_C - \beta_{LC}(t) L \epsilon, \\ \frac{dI_c}{dt} &= \gamma_C E_C - \mu_C(t) I_C, \\ \frac{dI_F}{dt} &= \beta_{CF}(t) I_C S_F - (\mu_F(t) + \eta_F) I_F \\ &\geq \beta_{CF}(t) I_C (N_F - \epsilon) - (\mu_F(t) + \eta_F) I_F, \\ &= -(\mu_F(t) + \eta_F) I_F + \beta_{CF}(t) I_C N_F - \beta_{CF}(t) I_C \epsilon, \end{aligned} \tag{A.21}$$

$$\begin{aligned} \frac{dE_D}{dt} &= \beta_{FD}(t) I_F S_D - (\mu_D + \gamma_D) E_D, \\ &\geq \beta_{FD}(t) I_F (N_D - \epsilon) - (\mu_D + \gamma_D) E_D \\ &= -(\mu_D + \gamma_D) E_D + \beta_{FD}(t) I_F N_D - \beta_{FD}(t) I_F \epsilon, \\ \frac{dI_{LD}}{dt} &= p_D \gamma_D E_D - (\mu_D + \eta_D) I_D, \\ \frac{dI_{HD}}{dt} &= (1 - p_D) \gamma_D E_D - (\mu_D + \sigma_D) I_{HD}, \\ \frac{dL}{dt} &= \theta_D(t)(1 - \phi_D) I_{LD} + \theta_D(t) I_{HD} - \mu_L(t) L, \end{aligned} \tag{A.22}$$

Hence we obtain $u'(t) \geq [F - V - \epsilon K]u(t)$ where $u(t)$, F and V are given by (A.2) and

$$\epsilon \cdot K = \epsilon \cdot \begin{bmatrix} 0 & 0 & 0 & 0 & 0 & 0 & \beta_{LC}(t) \\ 0 & 0 & 0 & 0 & 0 & 0 & 0 \\ 0 & \beta_{CF}(t) & 0 & 0 & 0 & 0 & 0 \\ 0 & 0 & \beta_{FD}(t) & 0 & 0 & 0 & 0 \\ 0 & 0 & 0 & 0 & 0 & 0 & 0 \\ 0 & 0 & 0 & 0 & 0 & 0 & 0 \\ 0 & 0 & 0 & 0 & 0 & 0 & 0 \end{bmatrix}. \tag{A.23}$$

Note that $R_0 > 1$ if and only if $\rho(\Phi_{F-V}(\omega)) > 1$. Thus, for $\epsilon > 0$ small enough, we have $\rho(\Phi_{F-V-\epsilon\cdot K}(\omega)) > 1$. Using Lemma A.1 and the comparison principle, we immediately obtain

$$\lim_{t\to\infty} E_C(t) = \infty, \quad \lim_{t\to\infty} I_C(t) = \infty, \quad \lim_{t\to\infty} I_F(t) = \infty, \quad \lim_{t\to\infty} E_D(t) = \infty,$$
$$\lim_{t\to\infty} I_{LD}(t) = \infty, \quad \lim_{t\to\infty} I_{HD}(t) = \infty, \quad \lim_{t\to\infty} L(t) = \infty,$$

which is a contradiction. Hence, M_0 is acyclic in M_∂, and P is uniformly persistent with respect to $(X_0, \partial X_0)$, which implies the uniform persistence of the solutions in the original system [37]. Consequently, the Poincaré map P has a fixed point $(\tilde{S}_C(0), \tilde{E}_C(0), \tilde{I}_C(0), \tilde{S}_F(0), \tilde{I}_F(0), \tilde{S}_D(0), \tilde{E}_D(0), \tilde{I}_{LD}(0), \tilde{I}_{HD}(0), \tilde{L}(0)) \in X_0$ with $\tilde{S}(0), \tilde{H}(0) \neq 0$. Thus, $(\tilde{S}_C(0), \tilde{E}_C(0), \tilde{I}_C(0), \tilde{S}_F(0), \tilde{I}_F(0), \tilde{S}_D(0), \tilde{E}_D(0), \tilde{I}_{LD}(0), \tilde{I}_{HD}(0), \tilde{L}(0)) \in \mathrm{Int}(\mathbb{R}^7_+)$ and

$$\begin{aligned}&(\tilde{S}_C(t), \tilde{E}_C(t), \tilde{I}_C(t), \tilde{S}_F(t), \tilde{I}_F(t), \tilde{S}_D(t), \tilde{E}_D(t), \tilde{I}_{LD}(t), \tilde{I}_{HD}(t), \tilde{L}(t)) \\ &= u(t, (\tilde{S}_C(0), \tilde{E}_C(0), \tilde{I}_C(0), \tilde{S}_F(0), \tilde{I}_F(0), \tilde{S}_D(0), \tilde{E}_D(0), \tilde{I}_{LD}(0), \tilde{I}_{HD}(0), \tilde{L}(0)))\end{aligned} \tag{A.24}$$

is a positive ω-periodic solution of the system.

Data availability

No data was used for the research described in the article.

References

[1] Boisson-Walsh A. Guinea worm disease inched closer to eradication in 2023. Lancet Infect Dis 2024;24(4):e224. http://dx.doi.org/10.1016/s1473-3099(24)00138-5.

[2] Casulli A. New global targets for NTDs in the WHO roadmap 2021–2030. PLoS Negl Trop Dis 2021;15(5):e0009373. http://dx.doi.org/10.1371/journal.pntd.0009373.

[3] Hopkins DR, Weiss AJ, Yerian S, Zhao Y, Sapp SG, Cama VA. Progress toward global dracunculiasis (guinea worm disease) eradication 2023–2024. MMWR Morb Mortal Wkly Rep 2024;73:991–8. http://dx.doi.org/10.15585/mmwr.mm7344a1.

[4] Garrett KB, Box EK, Cleveland CA, Majewska AA, Yabsley MJ. Dogs and the classic route of guinea worm transmission: an evaluation of copepod ingestion. Sci Rep 2020;10(1):1430. http://dx.doi.org/10.1038/s41598-020-58191-4.

[5] Boyce MR, Carlin EP, Schermerhorn J, Standley CJ. A one health approach for guinea worm disease control: scope and opportunities. Trop Med Infect Dis 2020;5(4):159. http://dx.doi.org/10.3390/tropicalmed5040159.

[6] Guagliardo SAJ, Wiegand R, Roy SL, Cleveland CA, Zirimwabagabo H, Chop E, et al. Correlates of variation in guinea worm burden among infected domestic dogs. Am J Trop Med Hyg 2021;104(4):1418–24. http://dx.doi.org/10.4269/ajtmh.19-0924.

[7] Wang Y, Perini T, Keskinocak P, Smalley H, Swann J, Weiss A. Evaluating the effectiveness of potential interventions for guinea worm disease in dogs in chad using simulations. Am J Trop Med Hyg 2023;109(4):835–43. http://dx.doi.org/10.4269/ajtmh.22-0654.

[8] Goodwin CE, L'echenne M, Wilson-Aggarwal JK, Koumetio SM, Swan GJ, Moundai T, et al. Seasonal fishery facilitates a novel transmission pathway in an emerging animal reservoir of guinea worm. Curr Biol 2022;32(4):775–82. http://dx.doi.org/10.1016/j.cub.2021.11.050.

[9] Gashirai TB, Musekwa-Hove SD, Lolika PO, Mushayabasa S. Global stability and optimal control analysis of a foot-and-mouth disease model with vaccine failure and environmental transmission. Chaos Solitons Fractals. 2020;132:109568. http://dx.doi.org/10.1016/j.chaos.2019.109568.

[10] Link K, Victor D. Guinea worm disease (dracunculiasis): opening a mathematical can of worms! bryn mawr college (M.Sc. Thesis), Bryn Mawr, PA; 2012, Available at: https://docslib.org/doc/7921321/guinea-worm-disease-dracunculiasis-opening-a-mathematical-can-of-worms.

[11] Adewole MO, Onifade AA. A mathematical model of dracunculiasis epidemic and eradication. IOSR J Math 2013;8(6):48–56. http://dx.doi.org/10.9790/5728-0864856.

[12] Smith RJ, Cloutier P, Harrison J, Desforges A. A mathematical model for the eradication of guinea worm disease. In: Mushayabasa S, Bhunu CP, editors. Understanding the dynamics of emerging and re-emerging infectious diseases using mathematical models. Kerala, India: Transworld Research Network; 2012, p. 133–56.

[13] Netshikweta R, Garira W. A multiscale model for the world's first parasitic disease targeted for eradication: guinea worm disease. Comput Math Methods Med 2017;2017:1473287. http://dx.doi.org/10.1155/2017/1473287.

[14] Losio AA, Mushayabasa S. Modeling the effects of spatial heterogeneity and seasonality on guinea worm disease transmission. J Appl Math 2018;2018:5084687. http://dx.doi.org/10.1155/2018/5084687.

[15] Ghosh I, Tiwari PK, Mandal S, Martcheva M, Chattopadhyay J. A mathematical study to control guinea worm disease: a case study on chad. J Biol Dyn 2018;12(1):846–71. http://dx.doi.org/10.1080/17513758.2018.1529829.

[16] Mushayabasa S, Losio A, Modnak C, Wang J. Optimal control analysis applied to a two-patch model for guinea worm disease. Eur J Appl Math 2020;70(1):1–23. http://dx.doi.org/10.58997/ejde.2020.70.

[17] Vinson JE, Park AW, Cleveland CA, Yabsley MJ, Ezenwa VO, Hall RJ. Alternative transmission pathways for guinea worm in dogs: implications for outbreak risk and control. Int J Parasitol 2021;51(12):1027–34. http://dx.doi.org/10.1016/j.ijpara.2021.05.005.

[18] Engelhard CAG, Hodgkins AP, Pearl EE, Spears PK, Rychtár J, Taylor D. A mathematical model of guinea worm disease in chad with fish as intermediate transport hosts. J Theoret Biol 2021;521:110683. http://dx.doi.org/10.1016/j.jtbi.2021.110683.

[19] Helikumi M, Mushayabasa S. Dog screening as a novel complementary guinea worm disease control tool to mitigate persistence in chad: a modeling study. Parasite Epidemiol Control 2023;23:e00328. http://dx.doi.org/10.1016/j.parepi.2023.e00328.
[20] Belsare A, Vanak A. Modelling the challenges of managing free-ranging dog populations. Sci Rep 2020;10(1):18874. http://dx.doi.org/10.1038/s41598-020-75828-6.
[21] Islam MR, Mir SA, Akash S. Dracunculiasis (guinea worm disease), a parasitic infection: epidemiology, life cycle, prevention, treatment, and challenges—correspondence. Ann Med Surg 2023;85:2264–5. http://dx.doi.org/10.1097/ms9.0000000000000670.
[22] Diekmann O, Heesterbeek JAP, Metz JAJ. On the definition and the computation of the basic reproduction ratio R0 in models for infectious diseases in heterogeneous populations. J Math Biol 1990;28(4):365–82. http://dx.doi.org/10.1007/bf00178324.
[23] Tayeh A, Sandy C, Cox FE. Guinea worm: from robert leiper to eradication. Parasitol 2017;144(12):1643–8. http://dx.doi.org/10.1017/s0031182017000683.
[24] Eichelberg H, Seine R. Life expectancy and cause of death in dogs. I. The situation in mixed breeds and various dog breeds. Berl Munch Tierarztl Wochenschr 1996;109(8):292–303, https://europepmc.org/article/med/9005839.
[25] Carmouze JP, Durand JR, Lévêque C. Lake chad: ecology and productivity of a shallow tropical ecosystem. Netherlands, Dordrecht: Monographiae Biologicae Springer; 1983, http://dx.doi.org/10.1007/978-94-009-7266-7.
[26] Sandy C, Ralph M, Nevio Z. Dracunculiasis and the eradication initiative: clinical microbiology reviews. Microbiol Rev 2002;15(2):223–46. http://dx.doi.org/10.1128/cmr.15.2.223-246.2002.
[27] Carlotti F, Nival S. Moulting and mortality rates of copepods related to age within stage: experimental results. Mar Ecol Prog Ser 1992;84:238–43. http://dx.doi.org/10.3354/meps084235.
[28] Cleveland CA, Eberhard ML, Thompson AT, Smith SJ, Zirimwabagabo H, Bringolf R, et al. Possible role of fish as transport hosts for dracunculus spp. larvae. Emerg Infect Dis 2017;23(9):1590. http://dx.doi.org/10.3201/eid2309.161931.
[29] Thiele EA, Eberhard ML, Cotton JA, Durrant C, Berg J, Hamm K, et al. Population genetic analysis of chadian guinea worms reveals that human and non-human hosts share common parasite populations. PLoS Negl Trop Dis 2018;12(10):e0006747. http://dx.doi.org/10.1371/journal.pntd.0006747.
[30] Moorthy VN. Observations on the development of dracunculus medinensis larvae in cyclops. Am J Hyg 1983;27:437–60. http://dx.doi.org/10.1093/oxfordjournals.aje.a118405.
[31] Marino S, Hogue IB, Ray CJ, Kirschner DE. A methodology for performing global uncertainty and sensitivity analysis in systems biology. J Theoret Biol 2008;254(1):178–96. http://dx.doi.org/10.1016/j.jtbi.2008.04.011.
[32] Molyneux D, Sankara D. Guinea worm eradication: progress and challenges—should we beware of the dog? PLoS Negl Trop Dis 2017;11(4):e0005495. http://dx.doi.org/10.1371/journal.pntd.0005495.
[33] Wang W, Zhao XQ. Threshold dynamics for compartmental epidemic models in periodic environments. J Dynam Differential Equations 2008;20(3):699–717. http://dx.doi.org/10.1007/s10884-008-9111-8.
[34] Posny D, Wang J. Computing the basic reproductive numbers for epidemiological models in nonhomogeneous environments. Appl Math Comput 2014;242:473–90. http://dx.doi.org/10.1016/j.amc.2014.05.079.
[35] Van den Driessche P, Watmough J. Reproduction numbers and sub-threshold endemic equilibria for compartmental models of disease transmission. Math Biosci 2002;180(1–2):29–48. http://dx.doi.org/10.1016/s0025-5564(02)00108-6.
[36] Smith HL, Waltman P. The theory of the chemostat: dynamics of microbial competition. Cambridge: Cambridge University Press; 1995, http://dx.doi.org/10.1017/CBO9780511530043.
[37] Zhao XQ. Dynamical systems in population biology. Springer; 2003, https://link.springer.com/book/10.1007/978-3-319-56433-3.